Anal. Chem. **2010,** *82,* 9275–9281

Label-Free Detection of Clustering of Membrane-Bound Proteins

Ixaskun Carton,[†] Alain R. Brisson,[§] and Ralf P. Richter*,[†]

Biosurfaces Unit, CIC biomaGUNE, Paseo Miramon 182, 20009 Donostia−San Sebastian, Spain, Max-Planck-Institute for Metals Research, Heisenbergstrasse 3, 70569 Stuttgart, Germany, and Laboratory of Molecular Imaging and Nanobiotechnology, IECB, UMR-5248 CBMN, CNRS-University Bordeaux 1-ENITAB, Avenue des Facultés, 33402 Talence, France

We report a new and label-free method to detect and characterize the clustering of membrane-bound proteins and, by extension, the lateral segregation of nanosized particles adsorbed to planar surfaces in liquid environment. The method exploits the contrast between two different mass and surface sensitive detection methods, quartz crystal microbalance with dissipation monitoring and ellipsometry. The time-resolved correlation of both techniques provides insight into subtle changes in the clustering state of surface-bound molecules that is not accessible with either technique alone. A theoretical model can provide quantitative predictions about the size of surface-bound clusters.

The organization of proteins at biological membranes is a vital feature of membrane bioactivity.[1] Notwithstanding significant progress, assessing the lateral organization of proteins and other nanosized objects on native and model membranes in their liquid environment remains a considerable challenge. The characteristic length scale of the objects under study is typically in the range of a few or a few tens of nanometers and can hence not be resolved with conventional light microscopic approaches. Scanning probe techniques, such as atomic force microscopy (AFM), provide the necessary lateral resolution, but the direct contact between probe and sample can severely perturb soft samples, and the limited scan speed of conventional AFMs renders the imaging of laterally mobile objects difficult or impossible.[2] Other techniques, such as Förster resonance energy transfer (FRET) or fluorescence correlation spectroscopy (FCS), require labeling of the sample.

Quartz crystal microbalance with dissipation monitoring (QCM-D) and ellipsometry, next to other optical mass-sensitive techniques, are now popular to study the formation of and morphological changes in soft films at the liquid−solid interface. These techniques average over a rather large surface area of micrometers or millimeters in extension and have thus a rather low, if any, intrinsic lateral resolution. Owing to the different transducer principles, however, surface-bound material generates a response in very different ways. QCM-D measures changes in the resonance frequency, Δf, and dissipation, ΔD, of a sensor crystal upon interaction of (soft) matter with its surface. The QCM-D response is sensitive to the mechanical properties of the surface-bound layer, and the masses (per unit area) that are measured with this technique include hydrodynamically coupled solvent.[3,4,19] Ellipsometry measures changes in the ellipsometric angles, Δ and Ψ, of polarized light upon reflection at a planar surface. The ellipsometric signal is sensitive to changes in the optical properties of the interface. For many biomolecular films, the changes in the refractive index at the interface can be translated into adsorbed masses,[5,6] which makes this technique suitable for the quantification of the adsorbed biomolecular mass. Hence, the mass measured by QCM-D includes a substantial amount of coupled water, whereas optical techniques measure the adsorbed biomolecular mass.[4] Here, we show that this contrast can be exploited to obtain information about the lateral segregation of membrane-bound proteins and, by extension, other nanoscale objects, at the nanometer scale.

To this end, we used the membrane-induced oligomerization of annexin A5 (AnxA5), a protein that is a popular marker of cell death (apoptosis), as a model system. AnxA5 binds in a calcium-dependent manner to membranes containing negatively charged lipids. The protein is monomeric in solution, but exhibits a strong tendency to assemble into trimers, when confined on a lipid

* To whom correspondence should be addressed. E-mail: rrichter@cicbiomagune.es. Phone: +34 943 0053 29. Fax: +34 943 0053 15.

[†] CIC biomaGUNE.

[‡] Max-Planck-Institute for Metals Research.

[§] CNRS-University Bordeaux 1-ENITAB.

(1) Song, L.; Hobaugh, M. R.; Shustak, C.; Cheley, S.; Bayley, H.; Gouaux, J. E. *Science* **1996**, *274*, 1859–1866. Geiger, B.; Bershadsky, A. *Curr. Opin. Cell Biol.* **2001**, *13*, 584–592. Bansal, D.; Campbell, K. P. *Trends Cell Biol.* **2004**, *14*, 206–213. Rosado, C. J.; Buckle, A. M.; Law, R. H.; Butcher, R. E.; Kan, W. T.; Bird, C. H.; Ung, K.; Browne, K. A.; Baran, K.; Bashtannyk-Puhalovich, T. A.; Faux, N. G.; Wong, W.; Porter, C. J.; Pike, R. N.; Ellisdon, A. M.; Pearce, M. C.; Bottomley, S. P.; Emsley, J.; Smith, A. I.; Rossjohn, J.; Hartland, E. L.; Voskoboinik, I.; Trapani, J. A.; Bird, P. I.; Dunstone, M. A.; Whisstock, J. C. *Science* **2007**, *317*, 1548–1551. Lingwood, D.; Simons, K. *Science* **2010**, *327*, 46–50.

(2) Richter, R. P.; Lai Kee Him, J.; Tessier, B.; Tessier, C.; Brisson, A. *Biophys. J.* **2005**, *89*, 3372–3385.

(3) Kanazawa, K. K.; Gordon, J. G., III *Anal. Chem.* **1985**, *57*, 1770–1771. Martin, S. J.; Frye, G. C.; Ricco, A. J.; Senturia, S. D. *Anal. Chem.* **1993**, *65*, 2910–2922. Domack, A.; Prucker, O.; Rühe, J.; Johannsmann, D. *Phys. Rev. E* **1997**, *56*, 680–689. Voinova, M. V.; Rodahl, M.; Jonson, M.; Kasemo, B. *Phys. Scr.* **1999**, *59*, 391–396. Urbakh, M.; Tsionsky, V.; Gileadi, E.; Daikhin, L. *In Piezoelectric Sensors*; Janshoff, A., Steinem, C., Eds.; Springer Verlag: Berlin, 2006; pp 111−150. Johannsmann, D.; Reviakine, I.; Rojas, E.; Gallego, M. *Anal. Chem.* **2008**, *80*, 8891–8889.

(4) Bingen, P.; Wang, G.; Steinmetz, N. F.; Rodahl, M.; Richter, R. P. *Anal. Chem.* **2008**, *80*, 8880–8890.

(5) De Feijter, J. A.; Benjamins, J.; Veer, F. A. *Biopolymers* **1978**, *17*, 1759–1772.

(6) Cuypers, P. A.; Corsel, J. W.; Janssen, M. P.; Kop, J. M. M.; Hermens, W. T.; Hemker, H. C. *J. Biol. Chem.* **1983**, *258*, 2426–2430.

10.1021/ac102495q
Published on Web 10/28/2010

membrane.[2,7,8] Under some conditions, AnxA5 does also form larger regular arrays. On silica-supported lipid bilayers, however, exclusively trimers have been found except at very high surface coverage.[2] Oligomerization can be impaired by selected amino acid mutations, while the secondary and tertiary structure and the membrane binding properties of the native protein remain preserved. As a second model system, we investigated the specific binding of the B-subunit of cholera toxin (CTB_5) to membranes containing the ganglioside GM1. CTB_5 is pentameric in solution and retains its oligomeric state upon binding to the membrane.[9]

MATERIALS AND METHODS

Buffer. A buffer solution of 10 mM HEPES, pH 7.4, and 150 mM NaCl in ultrapure water was used to prepare stock solutions of lipid vesicles. $CaCl_2$ (2 mM) was added for the formation of SLBs and protein binding assays. EGTA (2 mM) was added for the elution of AnxA5 from SLBs. All buffer components were purchased from Sigma.

Preparation of Lipids and Lipid Vesicles. Lyophilized dioleoylphosphatidylcholine (DOPC), dioleoylphospatidylserine (DOPS), and GM1 ganglioside (GM1) were purchased from Avanti Polar Lipids (Alabaster, AL). DOPC and DOPS were mixed in chloroform at a molar ratio of ~3:1. DOPC and GM1 were mixed in an equivolume mixture of chloroform and methanol at a molar ratio of ~19:1. The mixtures were dried, resuspended in buffer, and homogenized as described earlier.[10] Small unilamellar vesicles (SUVs) were obtained by sonication (30 min) with a tip sonicator (Branson), operated in pulsed mode at 30% duty cycle with refrigeration, followed by centrifugation (10 min at 14 000*g*) to remove titanium particles. SUV stock solutions had a concentration of ~1 mg/mL and were stored at 4 °C under nitrogen.

Expression and Purification of Proteins. Recombinant rat annexin A5 (AnxA5) was expressed in *Escherichia coli* BL21(DE3) cells and purified by Superdex-75 size exclusion column (Amersham Biosciences) followed by MonoQ HR5/5 anion-exchange chromatography, as previously described.[11] To produce the (R16E, R23E, K27E, K56E, K191E) AnxA5 mutant protein, the AGG, CGG, AAA, AAG, and AAG codons were replaced by GAG for R16E, R23E, K27E, K56E, and K191E, respectively. Mutations were verified by double-strand DNA sequence analysis. AnxA5 mut was expressed in *E. coli* BL21(DE3) cells and purified as previously described.[11] AnxA5 mut does not form trimers nor 2D arrays of trimers, yet binds PS-containing membranes similarly to wild-type AnxA5 (A. R. Brisson, unpublished results). Lyophilized pentameric B-subunit of cholera toxin (CTB_5) (Sigma) was reconstituted in ultrapure water. All protein stock solutions had a concentration of ~1 mg/mL and were stored at 4 °C.

Substrate Preparation. QCM-D sensors with a silica coating that was purpose-designed for ellipsometric measurements (QSX335, Q-Sense) were cleaned by immersion in a 2% sodium dodecyl sulfate solution for 30 min, rinsing with ultrapure water, blow-drying with nitrogen, and exposure to UV/ozone (BioForce Nanosciences, Ames, IA) for 30 min. Cleaned substrates were stored in air and again exposed to UV/ozone (30 min) prior to use.

***In Situ* Combination of Quartz Crystal Microbalance with Dissipation Monitoring and Ellipsometry.** Adsorption and interfacial processes were monitored simultaneously, by QCM-D and ellipsometry, on the same surface and in liquid environment, using purpose-designed fluid chambers. Two different fluid cells were employed: a closed fluid cell (Figure S1A) was provided by Q-Sense AB (Västra Frölunda, Sweden) and an open fluid cell (Figure S1B) was designed in our lab. The fluid cells were attached to a Q-Sense E1 setup, providing access to QCM-D data, and mounted on a spectroscopic rotating compensator ellipsometer (M2000V, Woollam, NE), providing access to ellipsometric data. QCM-D data, Δf and ΔD, were acquired at six overtones ($i = 3, 5, ..., 13$, corresponding to resonance frequencies of $f_i \approx 15, 25, ..., 65$ MHz) simultaneously, with subsecond time resolution. Ellipsometric data, Δ and Ψ, were acquired over a wavelength range from $\lambda = 380$ to 1000 nm, simultaneously, at 65° and 70° angle of incidence for the closed and open fluid cell, respectively, and with a time resolution of ~5 s. The working temperature was 23 °C.

Liquid Handling. Like in many other cases of biomolecular adsorption to surfaces,[12] mass-transport limitations strongly affect the binding of AnxA5 to SLBs.[2] QCM-D and ellipsometry inherently probe surface segments of different size,[13] and particular care is therefore required to avoid systematic errors in the correlation of QCM-D and ellipsometric data due to heterogeneous adsorption rates across the sensor surface. To this end, we adopted specialized liquid handling methods (see Supporting Information). To further validate our results, we employed two fluid cell designs (Figure S1, Supporting Information) with different liquid-handling schemes. The solvation curves from both setups coincided within experimental error (data not shown).

Quantification of Adsorbed Masses. Adsorbed masses from QCM-D data (including trapped solvent) were determined according to Sauerbrey's equation,[14] $m_{QCM} = -C\Delta f_i/i$, with the mass sensitivity constant $C = 18.06 \pm 0.15$ ng cm^{-2} Hz^{-1} for sensors with a resonance frequency of 4.95 ± 0.02 MHz. This equation is valid for films that exhibit low dissipation, as is the case for AnxA5, CTB_5, or SLBs. The experimental noise was typically below 2 ng/cm^2. It should be noted that the term "mass" in this work refers to adsorbed masses per unit surface area and that the unit is hence ng/cm^2.

Bound biomolecular masses were determined by numerical fitting of the ellipsometric data to a multilayer model. The data were fitted over the accessible wavelength spectrum, using the software CompleteEASE (Woollam). The model relates the measured ellipsometric responses, Δ and Ψ, as a function of λ,

(7) Oling, F.; Bergsma-Schutter, W.; Brisson, A. *J. Struct. Biol.* **2001**, *133*, 55–63.
(8) Govorukhina, N.; Bergsma-Schutter, A.; Mazères-Dubut, C.; Mazères, S.; Drakopoulou, E.; Bystrykh, L.; Oling, F.; Mukhopadhyay, A.; Reviakine, I.; Lai Kee Him, J.; Brisson, A. *In Annexins: Biological Importance and Annexin-Related Pathologies*; Bandorowicz-Pikula, J., Ed.; Landes Bioscience/Eurekah.com: Georgetown, TX, 2003; pp 37−55.
(9) Mou, J.; Yang, J.; Shao, Z. *J. Mol. Biol.* **1995**, *248*, 507–512. Brisson, A.; Bergsma-Schutter, A.; Oling, F.; Lambert, O.; Reviakine, I. *J. Cryst. Growth* **1999**, *196*, 456–470.
(10) Richter, R. P.; Mukhopadhyay, A.; Brisson, A. *Biophys. J.* **2003**, *85*, 3035–3047.
(11) Bérat, R.; Rémy-Zolghadry, M.; Gounou, C.; Manigand, C.; Tan, S.; Saltó, C.; Arenas, E.; Bordenave, L.; Brisson, A. R. *Biointerphases* **2007**, *2*, 165–172.
(12) Hermens, W. T.; Benes, M.; Richter, R. P.; Speijer, H. *Biotechnol. Appl. Biochem.* **2004**, *39*, 277–284.
(13) Edvardsson, M.; Svedhem, S.; Wang, G.; Richter, R.; Rodahl, M.; Kasemo, B. *Anal. Chem.* **2009**, *81*, 349–361.
(14) Sauerbrey, G. *Z. Phys.* **1959**, *155*, 206–222.

to the optical properties of the substrate, the adsorbed layer(s), and the surrounding solution. A five-layer model (solvent, biomolecular layer, silica, titania, titanium) was used. The SLB and the protein film were treated as a single biomolecular layer. We assumed this layer to be transparent and homogeneous (Cauchy medium), with a given thickness, d_{bml}, and a wavelength-dependent refractive index $n_{bml}(\lambda) = A_{bml} + B_{bml}/(\lambda/\mu m)^2$. B_{bml} was fixed to the value of the solvent ($B_{solvent} = 0.00322$),[15] while d_{bml} and A_{bml} were fitted simultaneously. The properties of all other layers were fixed to the values determined during calibration (see Supporting Information). The χ^2 value for the best fit was typically smaller than 3.0. The adsorbed mass per unit area was determined according to[5]

$$m_{optic} = \frac{d_{bml}^{(2)}(n_{bml}^{(2)} - n_{solvent}) - d_{bml}^{(1)}(n_{bml}^{(1)} - n_{solvent})}{dn/dc} \quad (1)$$

The indices (1) and (2) refer to determined values prior to and during a given incubation step, respectively. For most proteins, and within an error of less than 5%, the refractive index increment, dn/dc, is constant over the range of concentrations that are encountered within the biomolecular films in the reported measurements (0−500 mg/mL).[4] In eq 1, we employed the refractive indices of the biomolecular layers and the solvent ($n_{solvent} = 1.330$)[15] at $\lambda = 633$ nm and used a value of $dn/dc = 0.180$ cm^3/g for all proteins.[16] In practice, the errors associated with d_{bml} and $n_{bml} - n_{solvent}$ can be rather high for the nanometer-thin films investigated here. The errors are though covariant, i.e., the product $d_{bml}(n_{bml} - n_{solvent})$ and thus the adsorbed mass can be determined with good accuracy.[6] The experimental noise was typically below 1 ng/cm^2.

Quantification of Trapped Solvent. m_{optic} reflects the adsorbed biomolecular mass, while m_{QCM} includes trapped solvent. The fraction of trapped solvent, here also called solvation,[4] is then defined by $H = 1 - m_{optic}/m_{QCM}$. Reliable quantification of the trapped solvent was only possible for m_{optic} above ~35 ng/cm.[2] At lower coverages, minor heterogeneities in the mass transport to the sensor surface and transient perturbations of the QCM-D signal upon rapid sample injection had an appreciable influence on the solvation. These data were discarded.

Estimation of Film Thickness. For dense monolayers of globular proteins, the film thickness, i.e., the molecular dimensions of the adsorbed molecules in the direction of the surface normal, can readily be estimated from the masses determined from QCM-D and ellipsometry at maximal coverage.[17] From the conservation of mass and volume inside the film

$$m_{solvent} = m_{film} - m_{protein} = m_{QCM}^{max} - m_{optic}^{max} \quad (2a)$$

$$\frac{m_{film}}{\rho_{film}} = \frac{m_{protein}}{\rho_{protein}} + \frac{m_{solvent}}{\rho_{solvent}} \quad (2b)$$

and with the densities $\rho_{solvent} = 1.0$ g/cm^3 for aqueous solution and $\rho_{protein} = 1.35$ g/cm^3, one obtains

$$z = \frac{m_{film}}{\rho_{film}} = \frac{m_{QCM}^{max} - m_{optic}^{max}\left(1 - \frac{\rho_{solvent}}{\rho_{protein}}\right)}{\rho_{solvent}} \approx \left(\frac{m_{QCM}^{max}}{ng/cm^2} - 0.26\frac{m_{optic}^{max}}{ng/cm^2}\right) \times 0.01 \text{ nm} \quad (3)$$

RESULTS AND DISCUSSION

Combination of QCM-D and Ellipsometry to Monitor Biomolecular Adsorption. We employed an *in situ* combination of QCM-D and ellipsometry on the same surface to follow the formation of a supported lipid bilayer and subsequent binding of AnxA5. The design of the functionalized surface is schematically shown in Figure 1A, and representative QCM-D and ellipsometric data are shown in Figure 1B. The two-phase behavior together with the final changes in frequency and dissipation, $\Delta f = -26$ Hz and $\Delta D < 0.3 \times 10^{-6}$, upon incubation of SUVs are characteristic for the formation of an SLB of good quality.[18] The binding kinetics and additional frequency shifts of −18 and −17 Hz for native and mutant AnxA5, respectively, are in agreement with expectations for AnxA5 monolayers.[2,19] Very small changes in dissipation indicate tight association of the proteins with the SLB[20] and are characteristic for the membrane binding of AnxA5.[2,19] In the presence of $CaCl_2$, binding was fully irreversible, and AnxA5 could be fully eluted in EGTA, as expected.[2]

Adsorbed protein masses (Figure 1C) were derived from such QCM-D and ellipsometric data using established methods. The shape of the binding curves and the magnitude of the adsorbed masses are typical for the formation of a protein monolayer. The masses measured by QCM-D, m_{QCM}, were higher than the ellipsometric masses, m_{optic}, throughout the entire adsorption process, reflecting the additional contribution of solvent that is trapped in the film in a predominantly hydrodynamic manner.[4] From m_{QCM} and m_{optic} at maximal coverage, a thickness of 2.7 nm for native and mutant AnxA5 films can be estimated from eq 3, in good agreement with the protein's molecular dimensions.[19] The ellipsometric mass of 215 ng/cm^2, measured for native AnxA5 at saturation, was also close to expectations for the biomolecular mass of a dense protein monolayer.[19]

Apart from minor differences in the final adsorbed amount, the adsorption curves in Figure 1C appear very similar for both protein constructs, independent of the method that was used to monitor binding. The similarity confirms that the membrane binding properties of mutant and native AnxA5 are indeed quite similar. It illustrates also that very little, if any, information about the oligomerization or clustering state of the adsorbent can be inferred from the adsorption curves alone.

Trapped Solvent Provides Insight into Protein Clustering. Distinct differences became readily apparent after correlation of the masses that were derived from the two techniques (Figure

(15) Lide, D. R. *Handbook of Chemistry and Physics*, 85th ed.; CRC Press: Boca Raton, FL, USA, 2004; Daimon, M.; Masumura, A. *Appl. Opt.* **2007**, *46*, 3811–3820.

(16) Brandrup, J.; Immergut, E. H.; Grulke, E. A. *Polymer Handbook*, 3rd ed.; Wiley-Interscience: New York, 1989; Fasman, G. D. *Handbook of Biochemistry*; CRC Press: Cleveland, OH, 1973.

(17) Martin, S. J.; Frye, G. C.; Wessendorf, K. O. *Sens. Actuators A* **1994**, *44*, 209–218. Wolny, P. M.; Spatz, J. P.; Richter, R. P. *Langmuir* **2010**, *26*, 1029–1034.

(18) Richter, R. P.; Bérat, R.; Brisson, A. R. *Langmuir* **2006**, *22*, 3497–3505.

(19) Richter, R. P.; Brisson, A. *Langmuir* **2004**, *20*, 4609–4613.

(20) Johannsmann, D.; Reviakine, I.; Richter, R. P. *Anal. Chem.* **2009**, *81*, 8167–8176.

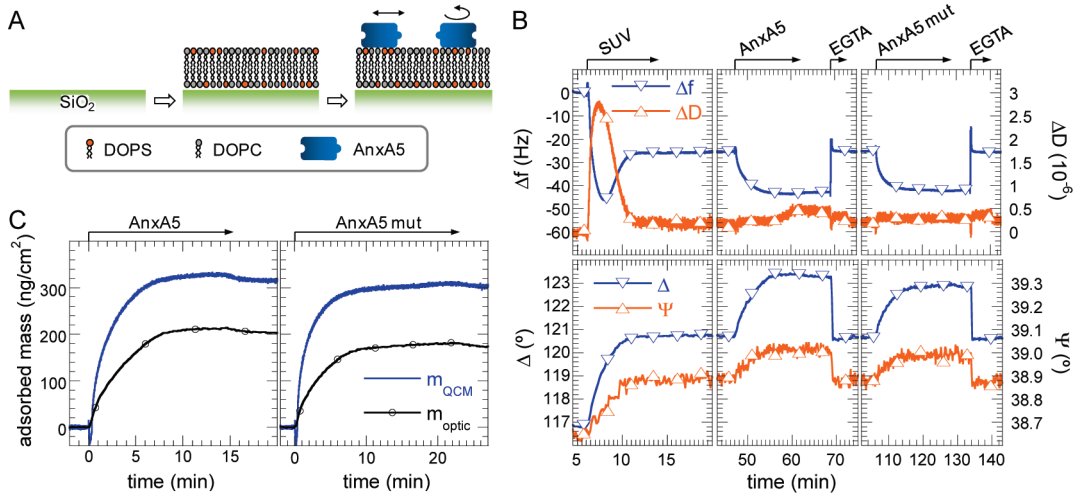

Figure 1. Binding of AnxA5 constructs to a supported lipid bilayer (SLB). (A) Schematic illustration of the immobilization strategy. The SLB was formed by spreading of small unilamellar vesicles containing DOPS and DOPC (molar ratio 1:3) on a silica surface. AnxA5 binds to negatively charged membranes in a Ca^{2+}-dependent manner. (B, top) Representative QCM-D data, $\Delta f/i$ and ΔD_i at $i = 11$, for the formation of an SLB (left), followed by binding and elution of AnxA5 (middle) and binding and elution of AnxA5 mut (right). (B, bottom) Representative ellipsometric data, Δ and Ψ, at $\lambda = 400$ nm, for the same measurement. Data were acquired with the closed fluid cell. Start and duration of sample incubation and elution by 2 mM EGTA are indicated (arrows). SUVs and proteins were incubated at concentrations of 50 and 10 μg/mL, respectively. Transient increases in Δf and decreases in ΔD during the first 30 s of sample incubation are artifacts that arise from rapid sample injection. (C) Kinetics of binding for AnxA5 (left) and AnxA5 mut (right) from solutions containing 7.5 μg/mL protein and 2 mM $CaCl_2$, derived from QCM-D (m_{QCM}) and ellipsometric (m_{optic}) data. Here, an open fluid cell was used.

2B). The relative contribution of the trapped solvent to the QCM-D response, $H = 1 - m_{optic}/m_{QCM}$, varied not only as a function of the protein's surface density but also between the two different AnxA5 constructs. Up to densities of ~150 ng/cm^2, the fractional trapped solvent for the nontrimerizing mutant was significantly higher than for the native protein.

The variations in H can be rationalized with a phenomenological model that we have proposed recently.[4] The model ascribes a solvation coat of given shape to each adsorbed molecule (Figure 2A). As the membrane becomes populated, the solvation coats of neighboring proteins increasingly overlap, thereby decreasing the amount of trapped solvent relative to the adsorbed biomolecular mass. From such a simple model, it is readily apparent that a given number of molecules would trap less solvent when being arranged into a two-dimensional cluster rather than randomly dispersed across a given surface area.

Fits to the Solvation Model. Solvation curves, i.e., plots of H as a function of m_{optic}, were compared to a theoretical model that relates the solvation curves to geometrical parameters (Figure 3A,B) of the adsorbent and its solvation coat and that accounts for the random distribution of adsorbents on the surface (model 3 in ref 4). Adsorbed particles are characterized by their height, z, and the half width, r, of their footprint, as well as their molecular weight, M_w, and their density, ρ. k_s is a measure for the lateral extension of the solvation coat. Here, we have approximated the solvation coat by a truncated cone (Figure 3B) rather than the truncated pyramid (Figure 3A) used previously.[4] This change was introduced to improve consistency with our simulation of random adsorbent distribution, by random sequential adsorption,[21] in which a circular footprint for the adsorbent was employed. Also, a circle is often a better approximation of the adsorbent's real footprint than a square. The modification of the solvation coat's shape has subtle consequences for the fitting which are described in the following.

To test the effect of shape on the outcome of the model, selected experimental data from ref 4 was fitted with a cone-shaped coat and compared with previously reported data for a pyramid-shaped coat (Figure 3C, Table 1). Here, r was fixed to the molecular dimensions of the adsorbent, while z and k_s were fitting parameters. The quality of the fit was good, independent of the coat's shape, in agreement with previous findings for other variations of the coat shape (including highly elongated shapes).[4] The derived values in z were marginally larger, by less than 3%, for the cone-shaped coat. An increase, by about 20%, though, was observed for k_s. This is not unexpected, given that the volume of a pyramid is substantially (about 27%) larger than that of a cone of the same height and width. For a given coat shape, k_s was only weakly dependent on the size and shape of the adsorbent (Table 1). For further fitting with the cone-shaped coat, we fixed $k_s = 1.35$.

Application of the Solvation Model to AnxA5. To apply the solvation model to the solvation curves for AnxA5 (Figure 2B), we assumed that the proteins assemble into oligomeric clusters of defined size (monomers, dimers, or trimers) that are distributed randomly on the membrane surface. M_w was set to 35.6, 71.2, or 106.8 kDa, respectively, corresponding to the weight of monomers, dimers, or trimers of AnxA5, and the density of the polypeptide chains was $\rho = 1.35$ g/cm^3. The protein height was fixed to $z = 2.7$ nm, in agreement with structural data[19,22] and with the independent estimation of the film thickness from m_{QCM} and m_{optic} at maximal coverage (see above). The cluster width remained the sole adjustable parameter. For the fit to the data at low coverage, we assumed a random adsorbent

(21) Adamczyk, Z.; Siwek, B.; Zembala, M.; Belouschek, P. *Adv. Colloid Interface Sci.* **1994**, *48*, 151–280.

(22) Swairjo, M. A.; Concha, N. O.; Kaetzel, M. A.; Dedman, J. R.; Seaton, B. A. *Nat. Struct. Biol.* **1995**, *2*, 968–974.

(23) Carton, I.; Malinina, L.; Richter, R. P. *Biophys. J.* In press.

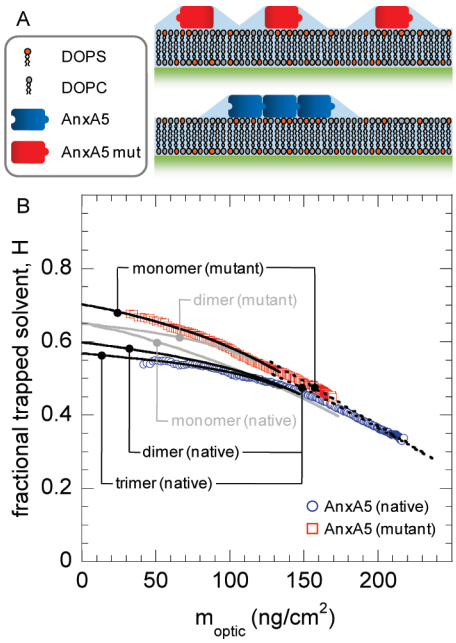

Figure 2. Solvation model and solvation curves. (A) Schematic presentation of membrane-bound proteins and their solvation coats (light blue), drawn approximately to scale. The relative contribution of trapped solvent to m_{QCM} decreases when adsorbed molecules segregate into clusters. (B) Representative solvation curves for the binding of native and mutant AnxA5 to SLBs. The curves differ distinctly at low but converge at high surface densities. Experimental variations in the solvation curve for a given AnxA5 construct did not exceed the size of the displayed symbols (not shown). Data were fitted by a model that assumes a cone-shaped solvation coat and random distribution of oligomeric clusters across the surface. Good fits (black solid lines) were obtained, when assuming that native and mutant AnxA5 are present as trimers and monomers, respectively. A dimer model could also fit the data for native AnxA5, although not as well as the trimer model. In contrast, no good fits (gray solid lines) could be found when assuming that the mutant is present as a dimer or the native protein as a monomer. The implementation of the random arrangement limits this model to biomolecular masses below ~135 ng/cm^2. At higher coverage, a simplified model that assumes cluster distribution in a regular hexagonal lattice (black dotted lines) fits the data well.

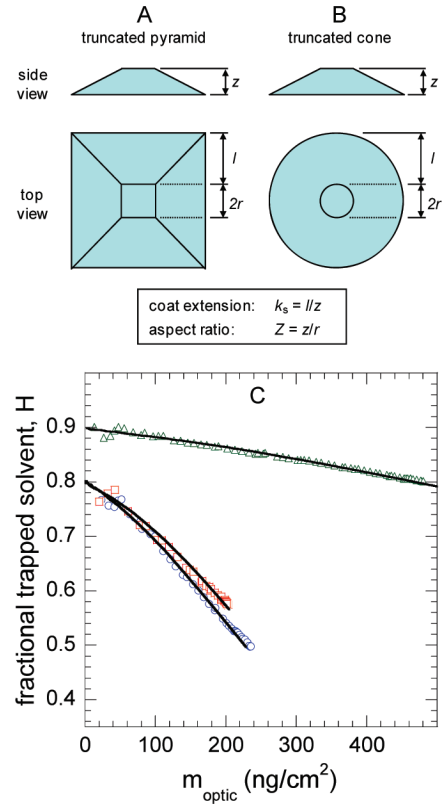

Figure 3. Shape of the solvation coat: truncated pyramid (A, employed previously)[4] and truncated cone (B, used in this study). The central cuboid (A) or cylinder (B), respectively, is thought to represent the dimensions of the adsorbed particle. Relevant parameters are annotated. (C) Best fits (black solid lines) of the solvation model, using the shape of a truncated cone for the solvation coat and assuming random adsorbent distribution, to experimental hydration curves from ref 4: adsorption of cowpea mosaic virus (CPMV) to gold (green triangles), streptavidin (SAv) on a biotinylated supported lipid bilayer (b-SLB) (blue circles), and avidin (Av) on a b-SLB (red rectangles). The model reproduces the solvation curves of all adsorbents well.

distribution (Figure 2B, solid lines). Our method of implementing such a distribution, the so-called random sequential adsorption,[21] limits the solvation model to fractional coverages below 54% (the so-called jamming limit). A simplified model, in which the adsorbent was assumed to be arranged in a regular hexagonal array, was used to estimate the solvation for higher fractional coverages (Figure 2B, dotted lines). At high coverage, the adsorbent distribution has only a minor effect on solvation,[4] and the estimate is hence expected to be good.

Results of the fitting are shown in Figure 2B and summarized in Table 2. For mutant AnxA5, the monomer model gave a good fit with a quality comparable to the reference data in Figure 3C. No good fit could be found for dimer or larger oligomer models. In contrast, the trimer model fitted the solvation curve for native AnxA5 best, again with a quality comparable to the reference data. No good fit could be found with the monomer model, while the dimer model still gave an acceptable fit. Our results were robust with respect to minor variations in the input parameters: fits of similar quality were obtained when the protein height was varied within the typical range of experimental uncertainty. A height change of 0.1 nm (or about 4%) affected the cluster width and footprint size by about 5% and 10%, respectively (data not shown). The widths for the monomer and the trimer (Table 2) agree well with the real size of AnxA5 oligomers.[7] The occupied surface area of 21−23 nm^2 per molecule is also in reasonable agreement with the surface area available per monomer in densely packed two-dimensional crystals of annexin A5 (25.5 nm^2 for $p3$ symmetry).[19]

Application of the Solvation Model to a Native Pentamer, Cholera Toxin B Subunit. In addition, we applied the solvation model to the binding of cholera toxin B subunit (CTB_5) on SLBs containing 5 mol % ganglioside GM1 (Figure 4).[23] The pentameric protein is roughly cylindrical and binds with one of the cylinder's planar faces to GM1-containing SLBs.[9] The cylinder has a height of 3.2 nm and a radius of 3.0 nm, but it is slightly tapered toward its membrane distal face.[24] For the fitting, we fixed the molecular weight at multiples of the weight of the monomeric subunit (11.6 kDa) and $\rho = 1.35$ g/cm^3. On the basis of structural data[24] and the independent estimation of the film thickness

(24) Zhang, R. G.; Westbrook, M. L.; Westbrook, E. M.; Scott, D. L.; Otwinowski, Z.; Maulik, P. R.; Reed, R. A.; Shipley, G. G. *J. Mol. Biol.* **1995**, *251*, 550–562.

Table 1. Parameters Used for Fitting the Solvation Model with Random Adsorbent Distribution to Experimental Hydration Curves

parameters		coat shape[a]	CPMV	SAv	Av
fixed[b]	M_w (kDa)	C, P	5400	60	66
	ρ (g/cm^3)	C, P	1.40	1.35	1.35
	r (nm)	C, P	14.0	2.7	3.0
fitted	z (nm)	C	26.5 ± 0.5	4.2 ± 0.1	4.5 ± 0.1
		P	26	4.1	4.4
	k_s	C	1.25 ± 0.15	1.45 ± 0.15	1.25 ± 0.15
		P	1.1	1.2	1.0
derived	$Z = z/r$	C	1.89	1.56	1.50
		P	1.86	1.52	1.47

[a] Results using a truncated cone (C, see Fig 4A) and a truncated pyramid (P, see ref 4) for the solvation coat are compared. [b] See ref 4 for details on the choice of the parameter values.

Table 2. Cluster Parameters Used for Fitting the Hydration Curves with the Solvation Model (Best Fits)

protein	monomers/ cluster	M_w/ cluster (kDa)	height (nm)	cluster width (nm)	area/ monomer (nm^2)
AnxA5 (native)	2	71.2	2.7	7.3 ± 0.2	20.9 ± 1.2
	3	106.8	2.7	9.3 ± 0.2	22.6 ± 1.0
AnxA5 (mutant)	1	35.6	2.7	5.4 ± 0.2	22.9 ± 1.7
CTB_5	5	58	3.2	5.7 ± 0.2	5.1 ± 0.4

from m_{QCM} and m_{optic} at maximal coverage, we set $z = 3.2$ nm. As for AnxA5, the data at low and high coverage was fitted by assuming random (Figure 4, solid lines) and regular (Figure 4, dotted line) adsorbent distribution, respectively.

The pentamer model provided a good fit (Table 2) with a value of $r = 2.85 \pm 0.1$ nm, in good agreement with the dimensions of CTB_5. Models with smaller oligomers (monomers, dimers, and trimers) systematically overestimated the hydration at low coverage. Larger oligomers (10-mer) underestimated the hydration at low coverage. Differences between the 10-mer and the pentamer fits were, though, smaller than those between the trimer and the pentamer fits, illustrating that the power to distinguish different oligomerization states decreases with increasing oligomer size.

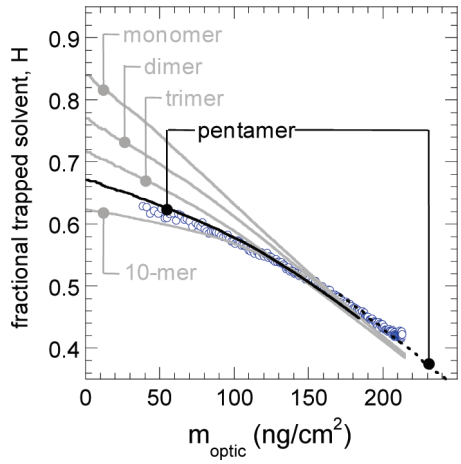

Figure 4. Representative solvation curve for binding of CTB_5 to a GM1-containing SLB. Experimental data (blue circles) were obtained with the closed fluid cell,[23] and experimental variations did not exceed the size of the displayed symbols. A fit assuming that CTB_5 is present as a pentamer (black solid line, random adsorbent distribution; black dotted line, regular adsorbent distribution at high coverage) reproduces the data well. Monomer, dimer, and trimer models (gray solid lines) clearly do not fit the data well. Significant deviations are also observed for the 10-mer model.

The quality of the fits and the agreement between the fitting parameters and the natural dimensions of AnxA5 and CTB_5 demonstrate that the combination of experimental solvation curves and the model can provide quantitative insight into the clustering state of surface-bound proteins. Importantly, the model can discriminate between different oligomerization states. The described fitting approach can be readily applied to proteins for which the cluster size is unknown. Most likely, the power to discriminative between the (predominant) presence of monomers, dimers, and higher oligomerization states will also be retained if clusters of different sizes are present simultaneously on the surface. Further investigation will be required to understand how a distribution of cluster sizes would affect the effectively measured cluster size.

What is the minimum information that needs to be known to safely argue on the lateral segregation of surface-bound nanoscale objects with the presented method? Our data on CTB_5 and AnxA5 indicate that the method is robust. k_s depends only weakly, if at all, on adsorbent size and aspect ratio, and this parameter can hence safely be fixed to 1.35. The density and molecular weight of the adsorbent are usually known. The height of the adsorbent also needs to be known. Fortunately, this information can typically be obtained from structural data or estimated from the masses at maximal surface coverage, as illustrated for CTB_5 and AnxA5. An intrinsic assumption of the model is that the adsorbent molecules/particles have a well-defined shape and that this shape does not change upon clustering. The model is best suited to investigate (globular) proteins with a well-defined ternary structure or other nanosized objects of defined shape. Hence, to safely argue on the lateral segregation, the orientation and (changes in) shape of the adsorbent should be reasonably well-known.

CONCLUSIONS AND PERSPECTIVES

We have demonstrated that solvation curves are highly sensitive to the lateral organization of molecules on the surface. Although neither QCM-D nor ellipsometry have an intrinsic lateral resolution on the nanometer-scale, the time-resolved correlation of both mass-sensitive techniques can provide quantitative insight into the organization of proteins on the molecular scale, without the need for labeling. A simple phenomenological model could

successfully reproduce our experimental data and is predictive in the sense that cluster formation can be detected, and estimates of the cluster size can be obtained. This novel analytical approach should be useful for the investigation of molecular processes at model membranes, in particular for the characterization of the organization and dynamics of membrane-bound or membrane-inserting proteins and membrane domains at the nanoscale. By extension, the method should also be of interest for the investigation of the organization of nanosized particles, including viruses or drug delivery vehicles, at surfaces in general.

ACKNOWLEDGMENT

Technical support by N. Heim (Bordeaux, France) and C. Gounou (IECB) is acknowledged. R.P.R. acknowledges funding from the German Federal Ministry of Education and Research (BMBF, project 0315157), the Spanish Ministry of Science and Innovation (MICINN, refs MAT2008-04192 and RYC2009-04275), and the Department of Industry of the Basque Government.

SUPPORTING INFORMATION AVAILABLE

Scheme of fluid cells and description of liquid handling methods; ellipsometric calibration of the fluid cells and the optical properties of the sensor coating. This material is available free of charge via the Internet at http://pubs.acs.org.

Received for review July 3, 2010. Accepted October 15, 2010.

AC102495Q